The Astrophysical Journal, 575:117–126, 2002 August 10

TWO-TEMPERATURE CORONAL FLOW ABOVE A THIN DISK

B. F. Liu
Yukawa Institute for Theoretical Physics, Kyoto University, Kyoto 606-8502, Japan; and Yunnan Observatory, Chinese Academy of Sciences, P.O. Box 110, Kunming 650011, China; bfliu@yukawa.kyoto-u.ac.jp

S. Mineshige
Yukawa Institute for Theoretical Physics, Kyoto University, Kyoto 606-8502, Japan

F. Meyer and E. Meyer-Hofmeister
Max-Planck-Institut für Astrophysik, Karl-Schwarzschild-Strasse 1, D-85740 Garching, Germany

and

T. Kawaguchi
Department of Astronomy, Faculty of Science, Kyoto University, Kyoto 606-8502, Japan
Received 2001 December 13; accepted 2002 April 10

ABSTRACT

We extended the disk corona model to the inner region of galactic nuclei by including different temperatures in ions and electrons as well as Compton cooling. We found that the mass evaporation rate, and hence the fraction of accretion energy released in the corona, depend strongly on the rate of incoming mass flow from the outer edge of the disk, a larger rate leading to more Compton cooling, less efficient evaporation, and a weaker corona. We also found a strong dependence on the viscosity, with higher viscosity leading to an enhanced mass flow in the corona and therefore more evaporation of gas from the disk below. If we take accretion rates in units of the Eddington rate, our results become independent of the mass of the central black hole. The model predicts weaker contributions to the hard X-rays for objects with higher accretion rate like narrow-line Seyfert 1 galaxies, in agreement with observations. For luminous active galactic nuclei, strong Compton cooling in the innermost corona is so efficient that a large amount of additional heating is required to maintain the corona above the thin disk.

Subject headings: accretion, accretion disks — galaxies: nuclei — X-rays: binaries — X-rays: galaxies

1. INTRODUCTION

It is commonly thought that active galactic nuclei (AGNs) are composed of a central supermassive black hole and a thin equatorial accretion disk. Spectral features of AGNs, the big blue bump, the soft X-ray excess and hard X-ray tails, and the 6.4 keV fluorescent iron lines show strong observational evidence for hot gas in the neighborhood of the inner accretion disk (e.g., Mushotzky, Done, & Pounds 1993; Zdziarski 1999). Soft disk photons are Compton up-scattered by the optically thin hot plasma and cause the power-law hard X-ray component in the spectrum. The relative strength of the hard X-ray component with respect to the UV–soft X-ray component, leading to the classification as soft or hard spectrum, is ascribed to the dominance of either the thermal emission from the accretion disk or of the thermal Comptonization in a hot plasma. The iron lines are explained by reflection of the hard X-rays from the underlying disk (e.g., Fabian et al. 2000; Reeves et al. 2001; Gondoin et al. 2001).

Theoretical simulations successfully reproduce the observed spectra by assuming a certain fraction of gravitational energy released in the hot gas (e.g., Haardt & Maraschi 1991; Kawaguchi, Shimura, & Mineshige 2001) and/or a certain spatial distribution of the hot gas (e.g., Merloni & Fabian 2001b). However, without understanding the coexistence of the disk and corona, the previous models require additional free parameters besides the mass of the black hole and the accretion rate for modeling the observed spectra.

On the other hand, mass evaporation from the underlying cool disk to the hot corona provides a mechanism for the change of the accretion disk in the outer region to the coronal flow/advection-dominated accretion flow (ADAF) in the inner region. Such a model (Meyer & Meyer-Hofmeister 1994; Meyer, Liu, & Meyer-Hofmeister 2000b) describes the physics of the process how mass and energy exchange and how the hot corona exists above the cool disk. Furthermore, the model allows self-consistent explanation of whether and where the accretion changes from the thin disk to the hot coronal flow/ADAF in dependence on the given accretion rate. The model explains the soft/hard spectral transitions in black hole X-ray binaries (Meyer, Liu, & Meyer-Hofmeister 2000a) and the truncation of the thin disk in soft X-ray transients and some galactic nuclei (Liu et al. 1999; Liu & Meyer-Hofmeister 2001). It provides a scenario for disk evolution and outburst cycles of soft X-ray transients (Meyer-Hofmeister & Meyer 1999). In these applications of the evaporation model the inner disk is truncated because of a relatively low accretion rate.

If we apply the disk corona model to AGNs, the inferred high-mass accretion rate in these luminous systems makes it possible for the disk to extend inward to the last stable orbit, since the high accretion rate tends to prohibit the disk from being depleted. Then the hard X-radiation originates from reprocessing in the hot corona. Such an inner corona has

very high temperature and low density; hence electrons and ions are no longer well coupled if all the heating goes to ions, and only Coulomb collisions transfer energy from ions to electrons. Photons from the thin disk are Compton up-scattered in the coronal region close to the central black hole. This process influences the coronal structure. Our former applications of the evaporation model adequate for equal ion and electron temperature (one-temperature coronae) would not be a good approximation anymore for the innermost regions of the black hole accretion system. A two-temperature treatment has to be developed.

Recently a semianalytical approach based on the same physics is carried out in detail by Różańska & Czerny (2000). In their investigation the corona is regarded as a layer with constant pressure, which means that the frictional heating is higher than that in the real corona, where the pressure scale height is much smaller as shown by our numerical computations (Meyer et al. 2000b). This approximation and further assumptions in their work lead to quite a difference in the detailed results. A recent investigation by Spruit & Deufel (2002) concerns the heating of the innermost disk region by hot ions and the resultant evaporation of matter from the disk.

In the present study we took into account the decoupling of electrons and ions and the Compton cooling, extending the previous disk evaporation model (Meyer et al. 2000b) to small distances from the black hole. We calculated the vertical structure of the corona numerically, attempting to describe the hot corona self-consistently in equilibrium with the cool disk below. We also investigated the dependence on the viscosity value chosen for the hot gas. We found that the evaporation efficiency is higher for larger viscosity, which means the mass flow in the corona is higher and, consequently, the mass accretion rate in the underlying disk is lower. Our new results are of interest with regard to the observed spectra and the spectral variations of AGNs and galactic black hole candidates. In § 2 we briefly describe the model. The detailed computational results are presented in § 3. In § 4 we discuss the dominant accretion form at different accretion rates and the possible coexistence of disk and corona in the innermost region of AGNs. Our conclusions are given in § 5.

2. THE MODEL

We consider a hot corona above a geometrically thin standard disk around a central black hole. Heat released by friction in the corona flows down into lower cooler and denser corona. There it is radiated away if the density is sufficiently high. If the density is too low, cool matter is heated up and joins the coronal gas. We call this process evaporation. This goes on until an equilibrium density is established. The gas evaporating into the corona still retains angular momentum; it will differentially rotate around the central object similar to a standard accretion disk. Because of friction the gas loses angular momentum and drifts inward, thus continuously draining mass from the corona toward the central object. This is compensated by a steady mass evaporation flow from the underlying disk. The process is driven by the gravitational potential energy released by friction in the form of heat in the corona. Therefore, mass is accreted to the central object partially through the corona (evaporated part) and partially through the disk (the left part of the supplying mass).

2.1. *The Equations*

In our earlier study (Meyer et al. 2000b) the equations for the corona above the disk are derived. The approximations used to describe the complex physics are discussed there in detail. For the application to coronae near the black hole we now, in addition, take into account different ion and electron temperatures and hence separate energy equations for ions and electrons. Compton cooling is also considered. We list the equations as follows:

Equation of state:

$$P = n_i \kappa T_i + n_e \kappa T_e = \frac{R\rho}{2\mu}(T_i + T_e) \ , \tag{1}$$

where we assumed a standard chemical composition ($X = 0.75,\ Y = 0.25$) for the corona. The average molecular weight is then $\mu = 0.62$. For simplicity we take the number density of ions n_i equal to that of electrons n_e, which is strictly true only for a pure hydrogen plasma.

Equation of continuity:

$$\frac{d}{dz}(\rho v_z) = \frac{2}{r}\rho v_r - \frac{2z}{r^2 + z^2}\rho v_z \ . \tag{2}$$

Equation of the z-component of momentum:

$$\rho v_z \frac{dv_z}{dz} = -\frac{dP}{dz} - \rho \frac{GMz}{(r^2 + z^2)^{3/2}} \ . \tag{3}$$

For the derivation of the above two equations, see equations (39) and (34) in Meyer et al. (2000b). The term $-[2z/(r^2 + z^2)]\rho v_z$ is due to the gradual change of the channel ($1 + z^2/r^2$, the channel cross section) of the ascending gas from a cylindrical to a spherical expanding shape at large height z.

There are now two energy equations (compare Meyer et al. 2000b, eq. [46] , for the one-temperature case), one for ions and one for electrons, and the cooling and heating processes in such a hot corona have to be included.

For ions, the energy balance is between viscous heating, cooling by collision with electrons, and radial and vertical advection:

$$\begin{aligned} &\frac{d}{dz}\left\{\rho_i v_z\left[\frac{v^2}{2} + \frac{\gamma}{\gamma - 1}\frac{P_i}{\rho_i} - \frac{GM}{(r^2 + z^2)^{1/2}}\right]\right\} \\ &\quad = \frac{3}{2}\alpha P\Omega - q_{ie} + \frac{2}{r}\rho_i v_r\left[\frac{v^2}{2} + \frac{\gamma}{\gamma - 1}\frac{P_i}{\rho_i} - \frac{GM}{(r^2 + z^2)^{1/2}}\right] \\ &\qquad - \frac{2z}{r^2 + z^2}\left\{\rho_i v_z\left[\frac{v^2}{2} + \frac{\gamma}{\gamma - 1}\frac{P_i}{\rho_i} - \frac{GM}{(r^2 + z^2)^{1/2}}\right]\right\} , \end{aligned} \tag{4}$$

where the radial velocity is approximated as $v_r \approx -\alpha V_s^2/\Omega r$ (V_s being sound speed). The friction is assumed to be proportional to the total pressure, and thus the viscous heating rate per unit volume is $q_{\rm vis} = (3/2)\alpha P\Omega$, as appears in the equation. Here we assume that all viscous heating goes to ions as usual (however, there is a controversy on possible viscous heating on electrons [e.g., Bisnovatyi-Kogan & Lovelace 1997; Quataert & Gruzinov 1999]), and the ion energy is transferred to electrons by Coulomb coupling

alone. Thus, the exchange rate of energy between electrons and ions for nonrelativistic approximation is (Stepney 1983)

$$q_{ie} = \left(\frac{2}{\pi}\right)^{1/2}\frac{3}{2}\frac{m_e}{m_p}\ln\Lambda\sigma_{\rm T}cn_en_i(\kappa T_i-\kappa T_e)\frac{1+T_*^{1/2}}{T_*^{3/2}}$$
$$= 3.59\times10^{-32}n_en_i(T_i-T_e)\frac{1+T_*^{1/2}}{T_*^{3/2}}\ , \quad (5)$$

with

$$T_* = \frac{\kappa T_e}{m_ec^2}\left(1+\frac{m_e}{m_p}\frac{T_i}{T_e}\right)\ ,$$

and G the gravitational constant, m_p and m_e the proton and electron mass, $\sigma_{\rm T}$ the Thomson scattering cross section, c the speed of light, κ the Boltzmann constant, and the Coulomb logarithm $\ln\Lambda$ taken as 20.

For electrons, the energy balance is determined by the processes of heating by collision with ions, cooling by Bremsstrahlung, Compton cooling, and vertical thermal conduction (the radial one is neglected since $\partial T_e/\partial r \ll \partial T_e/\partial z$), as well as advection.

$$\frac{d}{dz}\left\{\rho_ev_z\left[\frac{v^2}{2}+\frac{\gamma}{\gamma-1}\frac{P_e}{\rho_e}-\frac{GM}{(r^2+z^2)^{1/2}}\right]+F_c\right\}$$
$$= q_{ie}-n_en_iL(T_e)-q_{\rm Comp}$$
$$+\frac{2}{r}\rho_ev_r\left[\frac{v^2}{2}+\frac{\gamma}{\gamma-1}\frac{P_e}{\rho_e}-\frac{GM}{(r^2+z^2)^{1/2}}\right]$$
$$-\frac{2z}{r^2+z^2}\left\{\rho_ev_z\left[\frac{v^2}{2}+\frac{\gamma}{\gamma-1}\frac{P_e}{\rho_e}-\frac{GM}{(r^2+z^2)^{1/2}}\right]+F_c\right\}\ , \quad (6)$$

where $n_en_iL(T_e)$ is the bremsstrahlung cooling rate and $q_{\rm Comp}$ the Compton cooling rate,

$$q_{\rm Comp} = \frac{4\kappa T_e}{m_ec^2}n_e\sigma_{\rm T}c\frac{aT_{\rm eff}^4}{2}\ , \quad (7)$$

with $T_{\rm eff}$ the effective temperature of the main body of the disk,

$$T_{\rm eff}^4 = \frac{3GM\dot{M}_d}{8\pi r^3\sigma}\ .$$

Here we have added a factor of $\frac{1}{2}$ to the energy density of a blackbody photon field in equation (7) since photons from the underlying disks cover only half of the sky of electrons in the optically thin corona (compare with Rybicki & Lightman 1979) and F_c the thermal conduction (in Meyer et al. 2000b, eq. [49])

$$F_c = -\kappa_0T_e^{5/2}\frac{dT_e}{dz}\ , \quad (8)$$

where a is the radiative constant, σ is the Stefan-Boltzmann constant, $\kappa_0 = 10^{-6}$ g cm s^{-3} K$^{-7/2}$ for fully ionized plasma (Spitzer 1962), and $\dot{M}_d$ is the mass flow rate in the disk.

From equations (4) and (6) we obtain an energy equation in the same form as for our one-temperature model but with a new term for the Compton cooling,

$$\frac{d}{dz}\left\{\rho v_z\left[\frac{v^2}{2}+\frac{\gamma}{\gamma-1}\frac{P}{\rho}-\frac{GM}{(r^2+z^2)^{1/2}}\right]+F_c\right\}$$
$$= \frac{3}{2}\alpha P\Omega - n_en_iL(T_e)-q_{\rm Comp}$$
$$+\frac{2}{r}\rho v_r\left[\frac{v^2}{2}+\frac{\gamma}{\gamma-1}\frac{P}{\rho}-\frac{GM}{(r^2+z^2)^{1/2}}\right]$$
$$-\frac{2z}{r^2+z^2}\left\{\rho v_z\left[\frac{v^2}{2}+\frac{\gamma}{\gamma-1}\frac{P}{\rho}-\frac{GM}{(r^2+z^2)^{1/2}}\right]+F_c\right\}\ . \quad (9)$$

For convenience, the energy equations (4) and (9) are used in the numerical calculations instead of equations (4) and (6).

We want to point out that the one-zone approximation is taken for deriving the above equations. For a given distance r, we choose a region between r_1 and r_2 so that

$$\pi(r_2^2-r_1^2) = \pi r^2\ , \quad (10)$$

and

$$r = \frac{\int_{r_1}^{r_2}r'2\pi r'dr'}{\pi(r_2^2-r_1^2)}\ ; \quad (11)$$

i.e., $r_1 = 0.72r$ and $r_2 = 1.23r$. In the one-zone region the radial advection is taken related to the difference between mass inflow from the outer neighboring regions and outflow toward the inner neighboring regions,

$$\frac{(2\pi r\,\Delta z\rho v_r)_{r_2}-(2\pi r\,\Delta z\rho v_r)_{r_1}}{2\pi r\,\Delta z(r_2-r_1)} \approx -\frac{\rho v_r}{(r_2-r_1)} \approx -\frac{2}{r}\rho v_r\ . \quad (12)$$

This approximation for the net radial flow requires the mass outflow to be larger than the inflow. In the following sections we will see that the evaporation rate reaches a maximum and does not increase any more (see Fig. 3) inside the maximal evaporation region. This implies our results are inconsistent in the inner region, and we need to reconsider the radial flow. For this we study the radial flow more accurately in § 4.1. It turns out that the effect of the radial advective loss to the inner structures is very small; the corresponding terms in the continuity and energy equations are not very important. Therefore, our results based on one-zone approximation are still consistent.

2.2. *Boundary Conditions*

The differential equations (2), (3), (4), (8), and (9) contain five variables $P(z)$, $T_i(z)$, $T_e(z)$, F_c, and $\dot{m}(z)(\equiv\rho v_z)$, and can be solved with five boundary conditions.

At the lower boundary z_0 (the interface of disk and corona), there is no heat flux, and the temperature of the gas should be the effective temperature of the accretion disk. Former investigations (Liu, Meyer, & Meyer-Hofmeister 1995) showed that the coronal temperature increases from effective temperature to $10^{6.5}$ K in a very thin layer, and thus the lower boundary conditions can be reasonably approximated (Meyer et al. 2000b) as

$$T_e = 10^{6.5}\ {\rm K},\ T_i = T_e,\ \text{and}\ F_c = -2.73\times10^6P\ \text{at}\ z = z_0\ . \quad (13)$$

At infinity, there is no artificial confinement and hence no pressure. This requires sound transition at some height $z = z_1$, which is taken as our upper boundary. There is no heat flux from/to infinity either. We then constrain the upper boundary as

$$F_c = 0 \text{ and } v_z^2 = V_s^2 \equiv \frac{P}{\rho} = \frac{R}{2\mu}(T_i + T_e) \text{ at } z = z_1 \, . \quad (14)$$

With such boundary conditions, we have to assume lower boundary values for P and $\dot{m}$ to begin the integration along z; if the trial P and $\dot{m}$ fulfill the upper boundary conditions, we find the solutions.

3. COMPUTATIONAL RESULTS

We solved the differential equations (2), (3), (4), (8), and (9) using the Runge-Kutta method. The technical details of the integration procedure are similar to those in our previous study (Meyer et al. 2000b). In the present investigation, standard parameters were taken for the black hole mass $M = 10^8\ M_\odot$ and the viscosity coefficient $\alpha = 0.3$. The Compton cooling by photons depends on the radiation from the underlying disk and, hence, on the mass flow rate in the disk. This is an additional parameter on which the evaporation efficiency depends, and this parameter is different in different astrophysical objects. In order to study the coronal properties without involving the mass accretion rate in the disk, we first investigate the influence of viscosity without Comptonization, which means we assumed a very low mass accretion rate in the disk. The results are presented in §§ 3.1–3.5. The computational results for the effect of Compton scattering are discussed in § 3.6, the relevance for corona around stellar mass black holes in § 3.7.

3.1. *Vertical Structure of the Corona*

Figure 1 shows the vertical structure of the corona at distances $r = 3400r_g$ and $r = 340r_g$ (10^{16} cm for $M = 10^8\ M_\odot$), where $r_g = 2.95 \times 10^{13}(M/10^8\ M_\odot)$ cm is the Schwarzschild radius, and $T_{\rm vir} = GMm_p\mu/\kappa r = 3.37 \times 10^{12}(r/r_g)^{-1}$ K the virial temperature. The variation with height z of the variables, $P(z)$, $\dot{m}(z)$, $F_c(z)$, $T_e(z)$, $T_i(z)$, and V_z/V_s, is similar to that in our previous computations. The temperature, pressure, and density stay almost invariable in the corona from $z \sim r$ to the upper boundary ($z \lesssim 3r$). Steep changes occur in the lower corona ($z \lesssim r$), where the temperature increases from a chromospheric value ($T_e = T_i \approx 10^{6.5}$ K) to a coronal value [$T_i \sim (0.2\text{–}0.3)T_{\rm vir}$] and the pressure decreases rapidly. The density, $\rho \propto P/T$, drops even more steeply than temperature in the lower corona.

At a large distance $r \sim 3400r_g$ electrons in the corona are well coupled with ions, and thus electron and ion temperatures are nearly the same, $T_e \approx 10^8$ K. At a distance close to the black hole, Coulomb coupling between ions and electrons becomes weak because of low density and high temperature, and the temperature in ions (e.g., $T_i \approx 10^{11}$ K at $r = 10r_g$) is about 100 time higher than that in electrons.

3.2. *Distribution of the Temperature versus Distance*

Figure 2 shows the change of the coronal temperatures with distance. The ion temperature increases toward the central black hole, from values of about $\frac{1}{5}T_{\rm vir}$ in the outer region (e.g., $T_i \approx 1.8 \times 10^8$ K at $r = 3400r_g$) to $\frac{1}{3}T_{\rm vir}$ close to the black hole (e.g., $T_i \approx 10^{11}$ K at $r = 10r_g$), while the electron temperature hardly increases beyond the value of $T_e \sim 10^9$ K from the distance $r \sim 100r_g$ inward to the black hole. The temperature distribution of ions differs from that of electrons, since the viscous heat of ions can hardly be

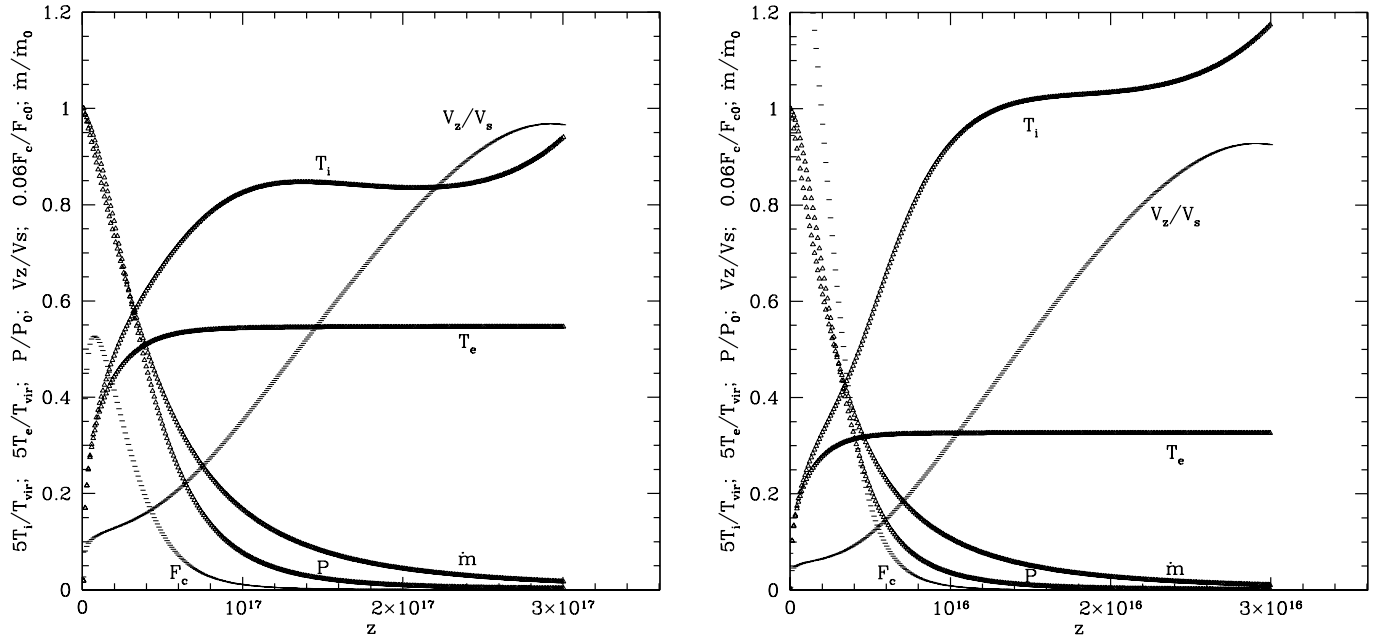

FIG. 1.—Vertical structure of the corona at different distances from a central black hole of mass $10^8\ M_\odot$ at $r = 3400r_g$(*left*) and $r = 340r_g$ (*right*). Distributions of the following quantities: Temperatures of ions T_i and electrons T_e in units of $0.2T_{\rm vir}$, ($T_{\rm vir}$ virial temperature); pressure P, thermal conductive flux F_c, and vertical mass flow $\dot{m} = \rho v_z$ scaled in their values at the lower boundary. Steep variations of P, T_i, T_e, and $\dot{m}$ occur in the lower layers with $z < r$; above these transition layers the corona is quasi-constant.

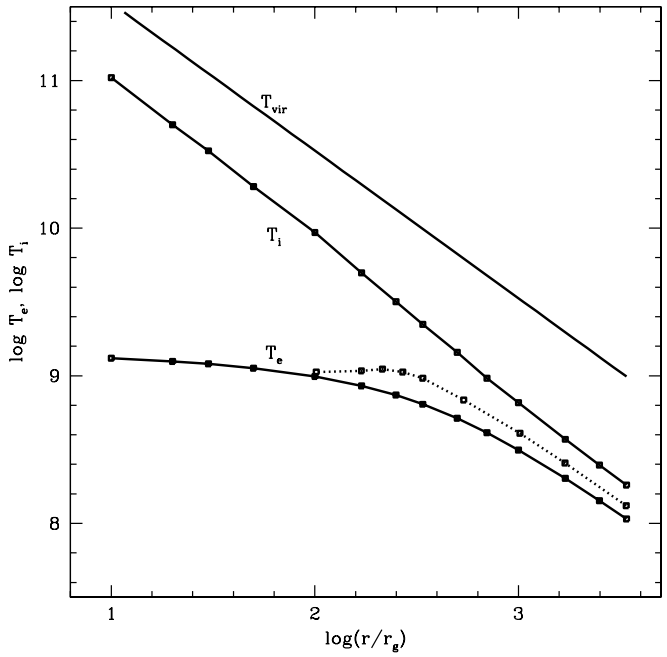

FIG. 2.—Temperature distribution vs. distance from the black hole. *Solid lines* (*from bottom to top*): Distributions of electron and ion temperature T_e and T_i, and virial temperature $T_{\rm vir}$, respectively. *Dotted line*: Temperature distribution of a 1-T model (Liu & Meyer-Hofmeister 2001). The ion temperature increases toward the central black hole; the electron temperature stays around 10^9 K in the inner region. The distribution resulting from the 2-T disk corona model is almost the same as that from a typical ADAF.

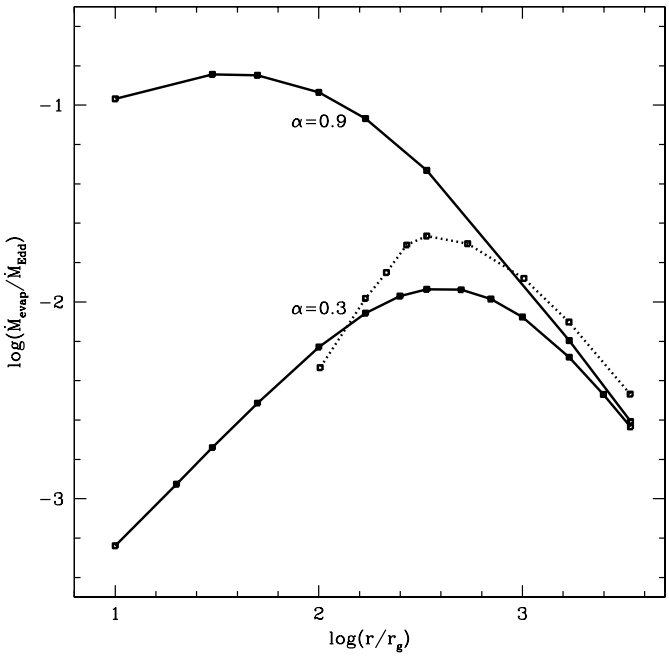

FIG. 3.—Evaporation rate vs. distance. *Solid lines*: Results from the 2-T model for a viscous coefficient $\alpha = 0.9$ (*upper line*) and $\alpha = 0.3$ (*lower line*). *Dotted line*: Result from the earlier computations using a 1-T model, $\alpha = 0.3$. The mass evaporation rate increases more than 10 times when the viscosity increases 3 times. The evaporation rate resulting from 2-T model is a little smaller than that from the 1-T model, since a small part of heat remains in ions to maintain a slightly higher temperature, and less heat goes to electrons (lower electron temperature) and is conducted downward for evaporation.

transferred by collisions to electrons and is only transferred to the entropy of ions. The fraction of heat turned into entropy becomes larger at small distances. The electrons, however, can efficiently cool by thermal conduction and radiation and, hence, keep their temperatures almost constant at decreasing distance in the inner region. Such distributions of ion and electron temperature versus distance in the corona are almost the same as those in a typical ADAF (Narayan & Yi 1995; Nakamura et al. 1997; Manmoto, Mineshige, & Kusunose 1997). The evaporation of mass is inefficient in the inner accretion region, and the viscous heat is transferred to entropy. The corona is essentially identical to an ADAF.

For comparison the temperature distribution resulting from our previous one-temperature (1-T) model is also plotted in Figure 2 (*dotted line*). From the outer regions to the distance of most efficient evaporation ($r \sim 340 r_g$), the 1-T temperature lies between the temperatures of ions and electrons of two-temperature (2-T) model; actually, the three temperatures are not much different. In the innermost region the one-temperature solutions are not adequate anymore unless there exists much more efficient coupling than Coulomb coupling.

3.3. *Distribution of Evaporation Rate versus Distance*

We define the mass evaporation rate from our one-zone region as $\dot{M}_{\rm evap}(r) \equiv 2\pi r^2 \dot{m}_0(r)$, where $\dot{m}_0(r)$ is the evaporation rate from unit surface area at the interface of the corona and the chromosphere (i.e., the lower boundary). Figure 3 shows the rate of mass evaporating from the disk to the corona versus distance. The evaporation rate $\dot{M}_{\rm evap}(r)$ increases with decreasing distance r, reaches a maximum (hump) of $\dot{M}_{\rm hp} = 0.012 \dot{M}_{\rm Edd}$ ($\dot{M}_{\rm Edd} = 10 L_{\rm Edd}/c^2$ being the Eddington rate) at $r_{\rm hp} \sim 340 r_g$, and decreases toward the black hole. The occurrence of the evaporation hump is an important characteristic of our disk corona model. The maximum of the coronal flow rate is caused by the change in the physical processes that remove the frictional heat. At large distances the coronal heat is balanced by the inward advection and wind loss. Downward heat conduction and subsequent radiation in the denser lower region play a minor role. Thus, the evaporation is weak. At small distances thermal conduction removes an increasing part of the viscous heat and becomes dominant with rising temperature. This downward-conducted viscous heat then evaporates the cool gas at the chromosphere and leads to efficient radiation. Therefore, the mass evaporation rate in the corona increases continuously with decreasing radius until the radius $r_{\rm hp}$ is reached. At distances $r < r_{\rm hp}$, the electrons are no longer well coupled with ions in the corona, and downward thermal conduction is less important; on the other hand, since the density increases toward the black hole, the heat at the lower coronal layer can easily be released by radiation in the innermost region, and thus evaporation is not active.

Also shown in Figure 3 (*dotted line*) is the distribution of the evaporation rate $\dot{M}_{\rm evap}(r)$ from our previous 1-T model ($\alpha = 0.3$). The maximum lies at the same distance from the black hole, but its value is 1 time larger than that of the 2-T model. The difference of evaporation efficiency between the 2-T and the 1-T model originates from the temperature difference; the slightly lower electron temperature in the 2-T model leads to less thermal conduction and resultant evaporation. A small part of the heat remains in ions to keep the

ion temperature slightly higher than the temperature in the 1-T model, instead of going to electrons and evaporating disk gas.

The gas evaporated from the disk into the corona flows inward through the corona toward the black hole, except for a small fraction leaving by wind. Therefore, the coronal mass flow rate at each distance r is the amount of gas evaporated from the disk at distances further outward up to r. Since the mass evaporation rate has a steep hump, the coronal flow at radius r outside the hump is approximately $\dot{M}_{\rm evap}(r)$, while at radius inside the hump, it is a little bit higher than the maximal evaporation rate $\dot{M}_{\rm hp}$.

3.4. *Energy Flows in the Corona*

For the local energy balance we consider the processes of viscous heating, radiative cooling, radial advection, and vertical advection (energy brought into the corona by gas evaporated from the disk and removed in the wind). Considering the coronal structure at a given distance r from the black hole, we integrate the energy loss by radiative cooling and the loss by vertical and sidewise advective outflow over z, the height of the corona. It is an interesting feature that these losses, normalized by the release of frictional energy, vary with distance r. We plotted the values in Figure 4. It shows that the fraction of viscous heat that is lost by radiation is larger at small distances than at large distances, while advection is dominant in the outer region ($r \sim 3400 r_g$). It takes away the major fraction of viscous heat there. At the distance $r \sim 340 r_g$, where evaporation rate reaches its maximum, advection and radiation both remove half of the viscous heat, respectively. In the inner region the density in the layers at the bottom of the corona is large; thus, the radiation becomes efficient and takes away a larger fraction of viscous heat than advection. This feature seems to be in contrast to the typical ADAFs, in which the flows are radiation-dominated farther out and become more and more advection-dominated with decreasing distance, until finally the advective cooling balances the viscous heating in the innermost region (Nakamura et al. 1997; Manmoto et al. 1997). But with a corona above the thin disk, evaporation leads to mass exchange, and therefore the flow is not a constant radial mass flow in the corona as in an ADAF.

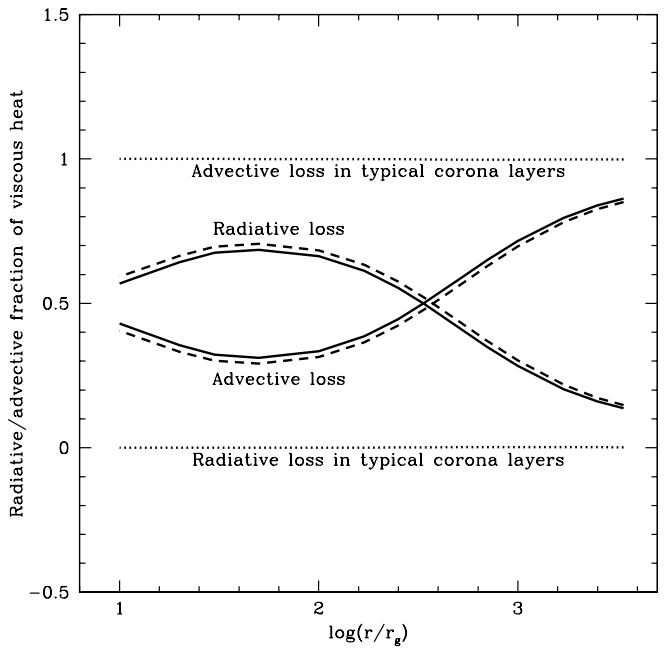

FIG. 4.—Variation of the energy losses with distance r from the black hole. Fraction of viscous heating going into radiation, and fraction removed by advection. *Solid lines*: Rates integrated over the total corona from the lower boundary (z_0, chromosphere) to the upper boundary (sound transition). *Dashed lines*: Rates integrated over the transition layer only, from z_0 to $z = r$. *Dotted lines*: Rates from $z = r$ to the upper boundary. The comparison of solid and dotted lines show that the processes in the lower coronal layers are responsible for the higher radiative loss fraction in the inner region and the lower advective loss fraction in the outer region. Considering the upper coronal layers only, the viscous heat almost flows inward as entropy with little radiation loss (a few $\times 10^{-3}$ in outer region), which is quite similar to the ADAFs.

The detailed calculations of the vertical structure allow the study of the difference in the energy flow in the upper corona as compared to that in the lower layers (compare also Meyer et al. 2000b, Fig. 4). Radiation and thermal conduction dominate the energy processes in the very low layer; the heat conducted downward by electrons and subsequently radiated away in the lower layers is provided by the viscous heat produced in the whole region from the chromosphere to a height of $z \sim r$. In the upper layers the pressure is very low, and the small amount of viscous heat produced there is almost completely advected. Thus, the total radiation (vertically integrated over the whole corona) predominantly originates from the lower coronal layers. Considering the layers from height $z = r$ to the upper boundary, the viscous heat is advected, as shown in Figure 4 (*dotted lines*). The very small fraction of radiative loss (e.g., a few $\times 10^{-3}$at $r \sim 3400 r_g$) decreases toward the black hole. In this sense, the corona is advection-dominated, consistent with the ADAF except that our corona model also includes vertical advection flow.

Comparing the energy flow in our computed corona with an ADAF, we find that the difference between the disk corona and the ADAF is in the supply of accretion gas. In the ADAF, accreting matter streams inward from the farther outward adjacent ADAF region, where the temperature is also high, while for the coronal flow above the disk, at $r > r_{\rm hp}$, the accreting mass is mainly supplied from the underlying disk with a temperature far lower than that in the corona, and the evaporating gas is heated to a high temperature before it accretes inward. This process needs to increase the entropy and the potential of the gas by "absorbing" viscous heat, and meanwhile the heat is partially radiated in the dense lower corona. If we consider the whole vertical region, the lower and upper coronal layers, the average temperature should be lower than that of an ADAF with the same mass supply rate, and the average radiative cooling is more efficient because of the structure of the lower coronal layers. After the essential increase of temperature and corresponding changes of the other quantities in the lower corona, the quantities are nearly constant in the upper layers, where the gas density is very low and the temperature is rather high. Such a corona is radiation-inefficient; almost all of the viscous heat is advected with the accretion flows (Fig. 4, *dotted lines*). These typical coronal layers are actually like an ADAF, which can also be seen from the temperature distribution shown in Figure 2.

3.5. *Effect of Viscosity*

The dependence of the evaporation rate on the viscosity is shown in Figure 3. We have chosen a relatively large viscous

coefficient, $\alpha = 0.9$, for comparison to the results for our standard value $\alpha = 0.3$. As already predicted by an earlier analytical study of this dependence, the influence on the evaporation efficiency is strong. For a larger viscosity in the corona, the evaporation rate is higher. The radial location of the maximal rate is shifted inward for higher viscosity values. The maximal rate for $\alpha = 0.9$ is $0.14\dot{M}_{\rm Edd}$, about 10 times larger than that for $\alpha = 0.3$, and the maximum occurs at a distance of about 30 Schwarzschild radii, about 10 times smaller than that for $\alpha = 0.3$. The reason is that the larger viscosity leads to more efficient heating and an enhanced mass flow in the corona. The increased viscous heat is then conducted downward by electrons and has to be radiated away by more efficient evaporation of the gas in the disk atmosphere. On the other hand, faster accretion in the corona tends to decrease more quickly the number density of the corona and requires more mass supply by evaporation to keep the energy balance at the interface of corona and disk. Therefore, the increase in viscosity largely increases mass evaporation. Similar results were obtained in an investigation using the 1-T model (Meyer-Hofmeister & Meyer 2001), where small viscosity is assumed.

As an important consequence of this dependence on viscosity, the distance where the mode of accretion via the thin disk changes to an ADAF is also affected. For a given mass inflow from the outer part, the disk can extend farther inward for smaller values of viscosity. Therefore, the emerging spectra should be different if two systems have a similar mass accretion rate but different viscosity in the hot coronal gas (for details see Meyer-Hofmeister & Meyer 2001). However, it is difficult to draw detailed conclusions from the observations.

3.6. *Effect of Compton Cooling*

At a small distance from the black hole, Compton cooling affects the structure of the corona. The Compton cooling term is included in the energy equation (9). Considering the processes that enter in the energy balance, Compton cooling is the only process that causes a dependence of the coronal structure on the accretion luminosity and, therefore, the mass flow in the underlying disk. Otherwise the equilibrium between corona and disk relies only on the existence of cooler gas below. The dependence on the mass flow in the disk adds one more parameter to the evaluation of coronal structure and the evaporation rate. To eliminate this problem we derived the results assuming a negligible Compton cooling (corresponding to very low mass flow rate in the disk) in the foregoing sections.

To investigate the effect of Compton cooling in a disk around a supermassive black hole with a mass of $10^8\ M_\odot$, we assumed a rate of $\dot{M}_{\rm in} = 0.05\ M_\odot\ {\rm yr}^{-1}$ ($\approx 0.02\dot{M}_{\rm Edd}$), corresponding to a bolometric luminosity $L = 2.8 \times 10^{44}$ ergs s^{-1} (assuming an energy-conversion coefficient of 0.1). A part of the mass flow goes to the corona through evaporation. So at a given distance the net mass flow rate in the disk should be

$$\dot{M}_d(r) = \dot{M}_{\rm in} - \dot{M}_c(r)\ , \qquad (15)$$

where $\dot{M}_c(r)$ is the integrated evaporation rate from outer edge to the distance r. This relation allows evaluation of the energy density of soft photons from the underlying disk to be scattered in the corona by assuming blackbody radiation. We calculated the coronal structure and the evaporation rate for different distances from large distance toward the central black hole. In Figure 5 the results for the assumed total mass flow rate $0.02\dot{M}_{\rm Edd}$ and $0.01\dot{M}_{\rm Edd}$ are shown together with the results without taking the Compton cooling into account (corresponding to a very low mass flow rate). As expected, the Comptonization has a strong influence on the structure of the corona if the mass flow rate in the disk is high. Since the mass flow rate at distance r in the disk depends on the evaporation in the further outward regions, whether the Compton cooling affects the evaporation rate at r depends on the accretion in the outward disk plus corona. At large distances, e.g., $r \sim 10^3 r_g$, the corona is hardly affected by Compton scattering, while in the inner region, Compton cooling is so strong that it overwhelms Bremsstrahlung and removes viscous heat efficiently, there is not much need for vertically advective cooling, and hence little gas evaporates from disk to corona. For the example with mass accretion rate $0.02\dot{M}_{\rm Edd}$ shown in this figure, the evaporation rate at $r = 340 r_g$ is half of the value without Comptonization and drops very steeply inward, reaching a value of $\sim$15 times less than the non-Compton one. In other words, strong Comptonization in the inner region restrains the evaporation. The corona then becomes rather weak.

An interesting feature caused by Compton cooling is the possible shift of the location of the maximal evaporation rate to a larger distance from the black hole. Computations for a series of mass flow rates show that from a larger total mass flow rate $0.02\dot{M}_{\rm Edd}$ to those for negligible mass flow in the disk, the evaporation rate at given r continuously increases, and location of the maximal evaporation moves inward, as shown in Figure 5. For a total mass flow rate

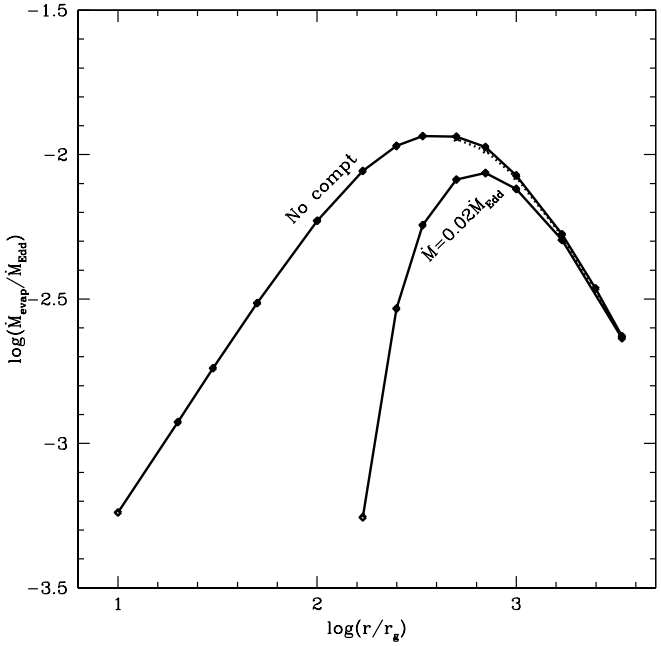

FIG. 5.—Effect of Compton cooling on the evaporation. *Upper solid line*: Evaporation rate without Comptonization (corresponds to a very low mass-flow rate in the thin disk). *Lower solid line and dotted line*: Evaporation rate including Compton up-scattering of soft photons from the disk with a total accretion rate of $\dot{M}_{\rm in} = 0.02\dot{M}_{\rm Edd}$ and $\dot{M}_{\rm in} = 0.01\dot{M}_{\rm Edd}$, respectively. The gas is partially evaporated into a coronal flow and partially accretes through the disk. The figure shows that the evaporation can be strongly restrained by Compton cooling, depending on the mass flow rate in the disk, in particular in the inner region.

from the outer regions of $\dot{M}_{\rm in} = 5.0 \times 10^{-4} \dot{M}_{\rm Edd}$, the Compton cooling does not affect the evaporation. For a rate $\dot{M}_{\rm in} = 0.01 \dot{M}_{\rm Edd}$, there is only very little influence by Compton cooling (see Fig. 5, *dotted line*); at the distance $r = 340 r_g$, where the evaporation rate is maximal, there is already not enough mass flow to supply the efficient evaporation. For a rate $0.02 \dot{M}_{\rm Edd}$ the changes are correspondingly larger, and the evaporation rate at $r = 340 r_g$ is small and already inside the location of the maximal evaporation rate that moved outward to a larger distance. In our previous papers (Liu et al. 1999; Meyer-Hofmeister & Meyer 1999) we suggested that the transition from the thin disk accretion to a coronal flow/ADAF is caused by the mass evaporation. The new results including Compton cooling by the disk radiation that show a decrease of the evaporation efficiency in the inner disk regions imply the transition in the accretion mode for a given mass flow rate in the disk (a rate below the maximal evaporation efficiency) at a smaller distance from the black hole. For higher rates the change between the hard and soft spectral states is expected, which occurs at a lower mass inflow rate than that without Compton cooling.

The effect of Comptonization obviously depends on the total mass accretion rate. Since large accretion flow in disk provides strong seed photons to be Compton scattered in the corona, the conductive heat at the lower layers of the corona can be appropriately released by Compton radiation; the evaporation will decrease or stop from some distance inward. At very large accretion rates, our computations show that the Compton cooling is so efficient that either sound transition at the upper boundary is inaccessible, or the corona needs artificial heat from the upper boundary; in other words, no evaporation solutions are found. This indicates that probably part of the coronal gas falls back to the disk by efficient Compton cooling in the innermost region.

3.7. *Corona around Stellar Mass Black Hole*

Since the physics of a disk corona around a stellar mass black hole is the same as that around a galactic black hole, we performed with the same code numerical calculations for accretion onto a stellar mass black hole of $M = 6\ M_\odot$ to study the influence of evaporation for adequate mass flow rates. We obtained similar results for both vertical and radial structure. If the distance is measured in Schwarzschild radius r_g and the mass accretion rate in Eddington rate, the radial distribution of the evaporation rate and the location of the maximum rate are the same as those for a supermassive black hole. The values of temperature at any distance (in Schwarzschild radii) for both systems are also the same. As for the vertical structure, the quantities are mass independent as long as we scale the size (distance r and height z) in Schwarzschild radius and multiply the quantities F_c, P, ρ, $\dot{m}$ by the mass of the black hole. This is essential since our equations and boundary conditions are invariant against scale transformations that leave temperature and velocities constant. Therefore, the coronal structures are scale free with respect to the mass of central black holes.

Dimensional analysis of the Compton cooling term and its related equations show that the coronal structures are still independent of the mass of the black hole even if the Compton cooling is included. This is easily understood by comparing the Compton cooling term and viscous heating term in the energy equation. If we scale the distance in Schwarzschild radius and the disk accretion rate in Eddington rate, we obtain the dependences of $q_{\rm vis}$ and $q_{\rm Comp}$ on the black hole mass as $q_{\rm vis} \propto P\Omega \propto PM^{-1}$, $q_{\rm Comp} \propto [T_e/(T_e + T_i)]PM^{-1}$. Obviously the Compton cooling term has the same dependence on M as the viscous term, implying that the results are also mass independent when Compton cooling is included. If we take the rate $0.01 \dot{M}_{\rm Edd}$ ($0.025\ M_\odot\ {\rm yr}^{-1}$ for a $10^8\ M_\odot$ black hole) as the upper limit for which the corona is not affected by Compton cooling (the true value should be slightly smaller, as shown in Fig. 5), we derive an accretion rate of $2.5 \times 10^{-10}\ M_\odot\ {\rm yr}^{-1}$ (or $9.5 \times 10^{16}\ {\rm g\ s}^{-1}$) for a $6\ M_\odot$ black hole for the limit. This rate is a little less than that expected for X-ray transients at spectral transition. This means the hard/soft spectral transition of X-ray transients is hardly affected by Compton cooling. The luminosity for which spectral transitions occur would be only slightly lower with Compton cooling included.

Despite the similarity between the corona above a stellar mass and that above a supermassive black hole (quantities scaled as described), the spectra would be different even if the mass accretion rates in unit of Eddington rate are the same. The reason is the different temperatures in the cool disk around the black holes. The situation is similar to that of the inner ADAFs with outer thin disks.

4. DISCUSSION

4.1. *Validity of the Approximation of Radial Advective Loss*

In § 2.1 we already pointed out the radial advection problem. For our computation of the coronal structure in a given zone of radial extent $r_2 - r_1 \approx 0.5r$, we assumed that the mass entering from outer adjacent region is less than the mass evaporating into this zone, and thus we approximated the radial mass loss $(1/r)(\partial r \rho v_r/\partial r) \approx -(2/r)\rho v_r$. Similar approximation was taken for the energy advection. Computations based on this one-zone model show that evaporation does not increase any more in the inner region. This means that our approximation is justified only for distances from the black hole larger than $r_{\rm hp}$. At smaller distances the mass flow in the corona should also include the mass entering from outer adjacent region besides the evaporation flow, and the radial advective loss has to be taken consistently with the mass flow change in the corona.

At a coronal region inside the hump, an inflow of $\sim \dot{M}_{\rm evap}(r_{\rm hp})$ superposes on the evaporation flow, increasing the coronal density and pressure. As a result, the gradient of radial mass flux $-(2/r)\rho v_r$, which is contributed by the evaporation mass in the one-zone region, should be formally decreased by a factor of $\eta(r)$ to compensate the increase of the density; i.e.,

$$\frac{1}{r}\frac{\partial r \rho v_r}{\partial r} \approx -\frac{2}{r}\eta(r)\rho v_r\ , \tag{16}$$

with

$$\eta(r) \approx \frac{\dot{M}_{\rm evap}(r)}{\dot{M}_c(r_2) + \dot{M}_{\rm evap}(r)}\ , \tag{17}$$

where $\dot{M}_c(r_2)$ is the mass flow coming from the outer edge of one-zone region and $\dot{M}_{\rm evap}(r)$ the mass flow evaporating into the one-zone region. The net energy flow is also multiplied by $\eta(r)$.

Computations have shown that the coronal flow comes mainly from the dominant evaporation region, i.e., the hump zone. As a rough estimate, we simplify $\eta(r)$ to

$$\eta(r) \approx \frac{\dot{M}_{\rm evap}(r)}{\dot{M}_c(r_{\rm hp})} \ . \tag{18}$$

Replacing $\dot{M}_{\rm evap}(r)$ in equation (18) by $2\pi r^2 \dot{m}_0(r)$, we recalculate the coronal structure with the new radial mass flux and energy flux; the evaporation rate along distance is plotted in Figure 6. From the figure we see that the evaporation by including the inflow from outer neighboring region is still inefficient in the inner region. The characteristic feature of hump-evaporation efficiency along distances does not change. Since η is very small at small distances far from the hump region, the dependence of the evaporation rate on the radial advective loss is quite weak. The coronal flow inside the hump is the same order of magnitude as the hump flow. The evaporation rate and the coronal flow seem to depend more strongly on the detailed cooling and heating processes, such as Comptonization and additional heating (large α). On this topic more consistent global investigations are needed, but they are beyond the scope of this paper.

4.2. *Accretion via Corona, Disk, or Both?*

We investigated the hot corona lying above a cool accretion disk and the mass and energy exchange between the corona and the disk. Mass continuously evaporates from the disk into the corona and flows in the corona toward the central black hole. At a large distance from the black hole only accretion via a thin disk occurs. Farther inward (at distances of 10^3–10^4 Schwarzschild radii for X-ray transients in quiescence or low-luminosity galactic nuclei), the accretion can change to the mode of an ADAF (e.g., Narayan, McClintock, & Yi 1996). This transition occurs where the evaporation rate exceeds the mass inflow rate in the cool disk. From that distance inward the thin disk is depleted, and the coronal flow fills the inward region up to the last stable orbit. Consequently, the accretion changes from thin disk outside to coronal flows/ADAFs inside. The transition radius is determined by the values of mass evaporation rate and mass flow rate in the disk. Actually, outside the transition radius both exist together, the cool disk and the corona above. Such a truncation of the thin disk only occurs if the mass supply rate in the disk is less than the maximal evaporation rate. If the mass inflow rate is higher, the disk cannot be fully depleted, and we expect an interior disk below the corona inside the distance of maximal evaporation. Summarizing these interactions, we claim that the mass supply rate $\dot{M}_{\rm in}$, compared to $\dot{M}_{\rm evap}$, determines whether accretion via the corona or the disk, or both dominate:

1. At low accretion rate $\dot{M}_{\rm in}$, a large part of the disk is depleted by mass evaporation and filled by coronal accretion flows/ADAFs, so accretion is dominated by hot coronal flows/ADAFs.
2. At a rate around the maximal evaporation rate, the disk truncation reaches its innermost possible distance, i.e., the hump distance, and an inner corona/ADAF coexists with an outer disk.
3. At a higher rate, the disk extends to the last stable orbit, and the corona, which is negligible in the far outward parts, could also be weak at the innermost region because of the efficient Compton cooling. In such a way, the thin disk exists at all distances with a corona lying above.

Up to now the evaporation model was applied to the situation of a thin disk truncated at a certain distance, that is, for mass flow rates $\dot{M}_{\rm in}$ less than the maximal $\dot{M}_{\rm evap}$ (Meyer et al. 2000a; Liu & Meyer-Hofmeister 2001). Now the new computation of coronal structure for inner regions and the evaporation efficiency there connect to the interesting question of how the radiation from these coronae with disks underneath affects the spectrum.

We have shown that the evaporation rate strongly depends on the viscosity value, especially that the maximum rate is changed, and this maximum rate occurs for the higher viscosity at smaller distance than for lower α. The larger the viscosity value, the smaller the inner region with an ADAF. Furthermore, the Compton cooling can affect the evaporation. If the mass flow rate $\dot{M}_{\rm in}$ is high, the Compton cooling reduces the evaporation, and because of the reduced maximal evaporation rate, the disk extends farther inward and may even extend to the last stable orbit. Therefore, the dominant accretion mode and the transition radius from outer disk accretion to an inner ADAF sensitively depend on both viscosity and mass supply rate to the disk. The dependence of the transition radius on the mass accretion rate is different from that in our previous investigation if Compton cooling becomes important.

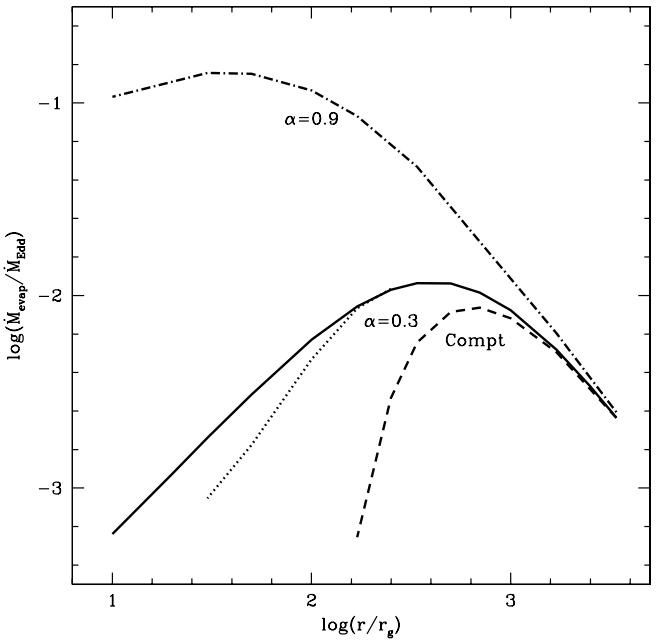

FIG. 6.—Influence of mass inflow from the hump region on the evaporation. *Solid line*: Basic case ($\alpha = 0.3$ without Compton cooling). *Dotted line*: Influence of hump flow. *Dashed line*: Influence of Comptonization. *Dash-dotted line*: Influence of α.

4.3. *Corona + Thin Disk in AGNs?*

In AGNs, hard X-ray tails and iron K_α lines are observed (e.g., Pounds et al. 1990; Matsuoka et al. 1990; Tanaka et al. 1995), implying that cold and hot gas exist in the vicinity of the central black hole. It is commonly believed that these components are the corona and disk, respectively. Soft pho-

tons from the disk are Compton up-scattered by energetic electrons in the optically thin corona and form the hard X-ray power-law spectral component. The iron lines are from the illumination of disk matter by X-ray radiations from the corona (e.g., Guilbert & Rees 1988; Lightman & White 1988; George & Fabian 1991).

The disk corona evaporation model shows that such kind of structure can exist self-consistently, if the mass accretion rate and the viscosity have appropriate values. Considering the high luminosity in AGNs, Comptonization is quite strong and the evaporation is restrained. Near the black hole, part of the coronal gas is expected to cool down and fall back to the disk. To keep the corona above the thin disk at this innermost region, very large viscosity is required, as is indicated in Figure 3. This implies that a large fraction of accretion energy needs to be released in the corona. Here we raise the same question as Merloni & Fabian (2001a) did, which is how the corona stores and releases so much energy.

In luminous AGNs (i.e., large $\dot{M}/\dot{M}_{\rm Edd}$) coronae cannot exist in the innermost region because Compton cooling is so strong that coronal plasma completely cools down and falls back to the disk. No strong hard X-ray spectral component is expected from the corona. This is consistent with the observational feature that high-$\dot{m}$ objects (e.g., narrow-line Seyfert 1 galaxies [NLS1s] with relatively small black hole mass) show steep hard X-ray spectra (e.g., Boller, Brandt, & Fink 1996; Brandt, Mathur, & Elvis 1997), while the relatively low luminosity AGNs (e.g., classical Broad- Line Seyfert 1s) show hard X-ray tails.

5. CONCLUSIONS

We have studied the properties of disk and corona around black holes, including the exchange of mass and energy between the disk and the corona. The decoupling of electron and ion temperatures and Compton cooling were taken into account. We found that the viscosity parameter α for the coronal gas has a strong influence on the evaporation efficiency; for larger α the mass flow in the corona increases, and the maximum of the evaporation rate is reached at a smaller radius. We also found that mass evaporation to the corona is largely restrained by Compton cooling at regions close to the black hole. Both effects, larger viscosity and smaller incoming mass accretion rate to the disk, lead to the coronal flow/ADAFs extending outward to a larger distance. Coronal radiation is weak for high accretion rates, consistent with the steep hard X-ray spectra observed in NLS1s and galactic black hole candidates. To maintain a corona lying above a thin disk down to the last stable orbit in an AGN, a large energy store/release in the corona is required. The results based on galactic nuclei are mass independent and, therefore, also applicable to black hole X-ray binaries.

B. F. L. and T. K. would like to thank the Japan Society for the Promotion of Science for support. This work is partially supported by the Grants-in Aid of the Ministry of Education, Science, Sports, and Culture of Japan (B. F. L., P.01020; S. M., 13640238; T. K., P.4616).

REFERENCES

Bisnovatyi-Kogan, G. S., & Lovelace, R. V. E. 1997, ApJ, 486, L43
Boller, Th., Brandt, W. N., & Fink, H. 1996, A&A, 305, 53
Brandt, W. N., Mathur, S., & Elvis, M. 1997, MNRAS, 285, L25
Fabian, A. C., Iwasawa, K., Reynolds, C. S., & Young, A. J. 2000, PASP, 112, 1145
George, I. M., & Fabian, A. C. 1991, MNRAS, 249, 352
Gondoin, P., Lumb, D., Siddiqui, H., Guainazzi, M., & Schartel, N. 2001, A&A, 373, 805
Guilbert, P. W., & Rees, M. J. 1988, MNRAS, 233, 475
Haardt, F.,& Maraschi, L. 1991, ApJ, 380, L51
Kawaguchi, T., Shimura, T., & Mineshige, S. 2001, ApJ, 546, 966
Lightman, A. P., & White, T. R. 1988, ApJ, 335, 57
Liu, B. F., & Meyer-Hofmeister, E. 2001, A&A, 372, 386
Liu, B. F., Yuan, W., Meyer, F., Meyer-Hofmeister, E., & Xie, G. Z. 1999, ApJ, 527, L17
Liu, F. K., Meyer, F., & Meyer-Hofmeister, E. 1995, A&A, 300, 823
Manmoto, T., Mineshige, S., & Kusunose, M. 1997, ApJ, 489, 791
Matsuoka, M., Piro, L., Yamauchi, M., & Murakami, T. 1990, ApJ, 361, 440
Merloni, A., & Fabian, A. C. 2001a, MNRAS, 321, 549
———. 2001b, MNRAS, 328, 958
Meyer, F., Liu, B. F., & Meyer-Hofmeister, E. 2000a, A&A, 354, L67
———. 2000b, A&A, 361, 175
Meyer, F., & Meyer-Hofmeister, E. 1994, A&A, 288, 175
Meyer-Hofmeister, E., & Meyer, F. 1999, A&A, 348, 154
———. 2001, A&A, 380, 739
Mushotzky, R. F., Done, C., & Pounds, K. A. 1993, ARA&A, 31, 717
Nakamura, K. E., Matsumoto, R., Kusunose, M.,& Kato, S. 1997, PASJ, 49, 503
Narayan, R., McClintock, J. E., & Yi, I. 1996, ApJ, 457, 821
Narayan, R., & Yi, I. 1995, ApJ, 452, 710
Pounds, K. A., Nandra, K., Steward, G. C., George, I. M., & Fabian, A. C. 1990, Nature, 344, 132
Quataert, E.,& Gruzinov, A. 1999, ApJ, 520, 248
Reeves, J. N., Turner, M. J. L., Pounds, K. A, O'Brien, P. T., Boller, Th., Ferrando, P., Kendziorra, E., & Vercellone, S. 2001, A&A, 365, L134
Różańska, A., & Czerny, B. 2000, A&A, 360, 1170
Rybicki, G. B.,& Lightman, A. P. 1979, Radiative Processes in Astrophysics, (New York: Wiley)
Spitzer, L. 1962, Physics of Fully Ionized Gases (2d ed.; New York: Interscience)
Spruit, H. C.& Deufel, B. 2002, A&A, in press
Stepney, S. 1983, MNRAS, 202, 467
Tanaka, Y., et al. 1995, Nature, 375, 659
Zdziarski, A. A. 1999, in ASP Conf. Ser. 161, High Energy Processes in Accreting Black Holes, ed. J. Poutanen & R. Svensson (San Francisco: ASP), 16